Key structural differences between green and red fluorescent proteins

Fluorescent proteins (FPs), indispensable tools in recent biological research, are exceptionally unique because their fluorophores are autocatalytically formed from the polypeptide chain. Most FPs discovered in nature are green fluorescent proteins (GFPs), which emit green fluorescence, while a smaller subset, red fluorescent proteins (RFPs), emit red fluorescence. The GFP fluorophore forms through the cyclization of three consecutive amino acids (Xaa-Tyr-Gly), creating an imidazolinone ring, followed by the formation of a double bond between the C_α and C_β atoms of the Tyr residue. This series of reactions requires one molecule of oxygen [1]. In the case of RFP, an additional oxidative step occurs, leading to the formation of an N-acylimine, absent in GFP fluorophores, which extends the π conjugation system in the fluorophore and shifts the absorbance and fluorescence to a longer wavelength (Fig. 1) [2-4]. Therefore, one extra molecule of oxygen is required for the formation of the RFP fluorophore.

There is a high demand for high-performance RFPs for their use in multi-color labeling and their advantage in deep tissue imaging. Converting GFP into RFP through mutagenesis could significantly contribute to developing novel RFPs, but such attempts have so far been unsuccessful. Moreover, the mechanisms by which GFPs and RFPs achieve distinctly different autocatalytic reactions while sharing similar overall structure remain poorly understood.

Our recent study successfully engineered GFPs into red and revealed key structural differences between GFP and RFP [5]. First, we focused on the differences between AzamiGreen (AG), a GFP derived from stony coral, and three representative RFPs—DsRed, eqFP578, and eqFP611. By introducing amino acid residues highly conserved among the three RFPs into AG and combining this with site-directed saturation mutagenesis, we successfully converted this GFP into an RFP (Figs. 2(a,b)). Notably, this novel RFP, named AzamiRed1.0 (AR1.0), exhibited a high fluorescence quantum yield of 0.65, among the highest for RFPs with fluorescence wavelengths exceeding 600 nm. The sequence difference between AG and AR1.0 was only 29 amino acids, making it the closest GFP-RFP pair. We determined the three-dimensional structures of AG and AR1.0 by collecting X-ray diffraction data at SPring-8 **BL41XU** to investigate the mechanisms of forming the distinct GFP and RFP fluorophores.

Strikingly, it was revealed that the multiple mutations introduced in AR1.0 cooperatively contributed to significant rearrangements in the interaction networks around the fluorophore (Figs. 2(c,d)). For example, a new hydrogen bond network formed in AR1.0, extending from the main chain nitrogen of Ala67 through Thr107 and the side chain of Gln105 to the main chain oxygen of Gln60. The hydrogen bond between the Asn65 side chain and the Tyr87 hydroxyl group in AG was absent in AR1.0, where residue 65 was substituted with Ser and residue 87 with Phe. Instead, the Ser65 side chain of AR1.0 formed a hydrogen bond with the hydroxyl group of Tyr116. Additionally, the hydroxyl group of Thr69 in AG formed a hydrogen bond with the guanidino group of Arg66, assisting its interaction with the Glu211 side chain. In AR1.0, however, Arg66 and Thr69 were replaced with Lys and Ile, respectively, leading to a new interaction between Lys66 and Glu144. Due to these structural changes, a cavity absent in AG appeared in AR1.0

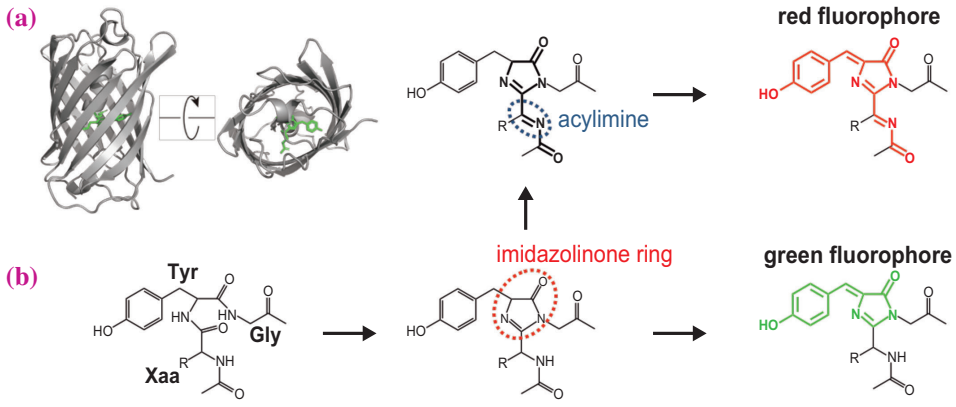

Fig. 1. Fluorophore of fluorescent proteins. **(a)** Structure of a fluorescent protein. **(b)** Proposed scheme of fluorophore formation in GFP and RFP.

near the fluorophore (Figs. 2(e,f)). A similar cavity was also observed in other RFPs. Interestingly, while water molecules occupied this cavity in the AR1.0 structure, glycerol and acetate molecules used for crystallization were found in the cavities of eqFP578 and eqFP611 structures, respectively, indicating that the cavity is accessible from outside the protein. As mentioned above, red fluorophore formation requires one additional molecule of oxygen, which must enter the vicinity of the fluorophore. This cavity would allow the entry of the oxygen molecule necessary for red fluorophore formation, although further verification is needed.

In addition to the cavity, the protonation state of the Tyr63, the core residue of the fluorophore, also seems to be important for the formation of RFP fluorophores. As a result of the M159K mutation in AR1.0, the side chain amino group of Lys159 into close proximity with the phenolic hydroxyl group of the fluorophore, suggesting that the phenolic hydroxyl group of Tyr63 is stabilized in its deprotonated state in AR1.0. When Lys159 in AR1.0 is reverted to Met, a mixture of red and green fluorophores is formed, underscoring the critical role of Tyr63 deprotonation.

AR1.0 formed a homo-tetramer, like its precursor AG. Because monomeric FPs are generally preferred as a fluorescent tag, we constructed a monomeric AR1.0 variant named mARs1. While mARs1 exhibited a reduced quantum yield of 0.26 compared to AR1.0, its fluorescence was sufficiently bright for live cell imaging. When expressed in cells as fusion constructs with various proteins or localization tags, mARs1 localized to expected cellular locations, including mitochondria, Golgi apparatus, lysosomes, actin filaments, and microtubule plus ends, demonstrating its utility for visualizing these structures.

Previously, new RFPs were obtained only by isolating new proteins from nature or modifying existing RFPs. However, isolating new RFPs from nature is challenging, and the limited sequence diversity of existing RFPs constrains the development of high-performance variants. Our study demonstrates that the artificial conversion of GFP to RFP offers a promising alternative approach, significantly enhancing the sequence diversity of RFPs. Additionally, our findings provide structural insights into the mechanisms underlying red fluorophore formation in RFPs.

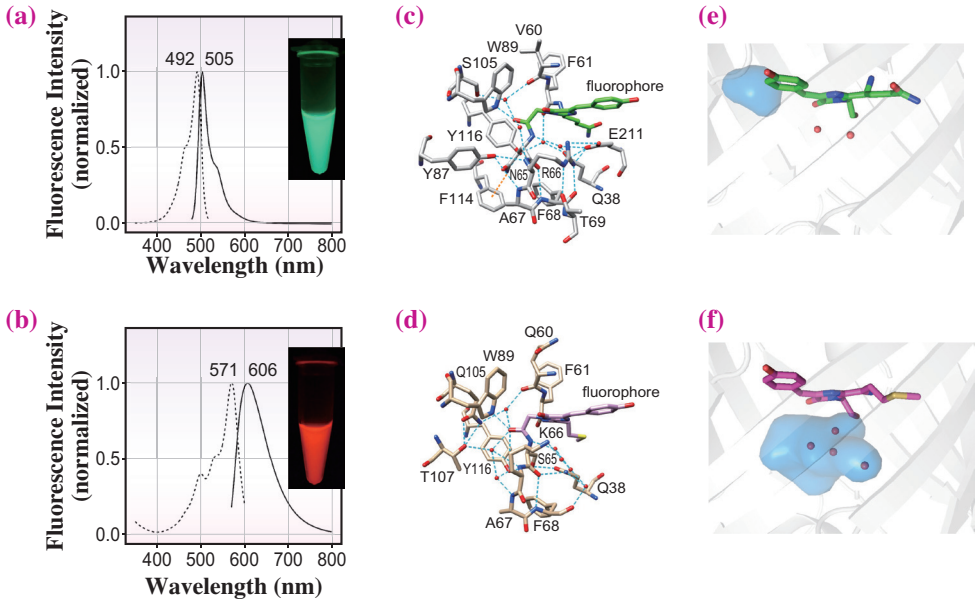

Fig. 2. Spectroscopic and structural difference between AG (upper panels) and AR1.0 (lower panels). **(a,b)** Excitation (dot) and emission (solid) spectra and fluorescence photographs of purified FPs. **(c,d)** Interaction networks near the fluorophore. **(e,f)** Cavities near the fluorophore.

Hiromi Imamura[a,*] and Katsumi Imada[b]

[a] Organization of Research Initiatives, Yamaguchi University
[b] Graduate School of Science, Osaka University

*Email: imamura-h@yamaguchi-u.ac.jp

References

[1] R. Y. Tsien: Annu. Rev. Biochem. **67** (1998) 509.
[2] L. A. Gross *et al.*: Proc. Natl. Acad. Sci. USA **97** (2000) 11990.
[3] S. Pletnev *et al.*: J. Am. Chem. Soc. **132** (2010) 2243.
[4] R. L. Strack *et al.*: J. Am. Chem. Soc. **132** (2010) 8496.
[5] *H. Imamura, S. Otsubo, M. Nishida, N. Takekawa, K. Imada: Proc. Natl. Acad. Sci. USA* ***120*** *(2023) e2307687120.*